RGD Cyclopeptide Equipped with a Lysine-Engaging Salicylaldehyde Showing Enhanced Integrin Affinity and Cell Detachment Potency

Journal Article

Author(s):
Sacco, Giovanni; Arosio, Daniela; Paolillo, Mayra; Gloger, Andreas; Scheuermann, Jörg; Pignataro, Luca; Belvisi, Laura; Dal Corso, Alberto; Gennari, Cesare

Publication date:
2023-04-03

Permanent link:
https://doi.org/10.3929/ethz-b-000604148

Originally published in:
Chemistry - A European Journal 29(19), https://doi.org/10.1002/chem.202203768

Chemistry–A European Journal
Research Article
doi.org/10.1002/chem.202203768
Chemistry Europe
European Chemical Societies Publishing
www.chemeurj.org

RGD Cyclopeptide Equipped with a Lysine-Engaging Salicylaldehyde Showing Enhanced Integrin Affinity and Cell Detachment Potency

Giovanni Sacco,[a] Daniela Arosio,[b] Mayra Paolillo,[c] Andreas Gloger,[d] Jörg Scheuermann,[d] Luca Pignataro,[a] Laura Belvisi,[a] Alberto Dal Corso,*[a] and Cesare Gennari*[a]

Abstract: Salicylaldehyde (SA) derivatives are emerging as useful fragments to obtain reversible-covalent inhibitors interacting with the lysine residues of the target protein. Here the SA installation at the C terminus of an integrin-binding cyclopeptide, leading to enhanced ligand affinity for the receptor as well as stronger biological activity in cultured glioblastoma cells is reported.

Introduction

Covalent ligands are synthetic small molecules whose binding to a specific protein involves the formation of a covalent bond between an electrophilic group in the ligand and a nucleophilic residue in the protein counterpart. The pharmaceutical use of covalent ligands as protein inhibitors has been widely explored to increase i) drug potency (resulting from a strong drug-protein binding), ii) long-lasting pharmaceutical effects (resulting from a long "residence time" of the drug in the protein binding site) and iii) target specificity (resulting from the formation of an array of both non-covalent and covalent binding interactions).[1] In this context, reversible-covalent (RC) ligands are receiving increasing attention[2] and most of those developed to date can react with the thiol groups of cysteine (Cys) residues.[3] While Cys is one of the least common amino acids in proteins, lysine (Lys) is highly abundant in the proteome and one of the most frequent residues on the outer structural layers of proteins.[4] For these reasons, the ligand derivatization with aldehyde tags capable of imine bond formation with Lys ε-amino groups can dramatically expand the RC ligands applications. In recent years, *ortho*-formyl phenylboronic acids have become a standard in this field, due to the high stability towards hydrolysis of the resulting iminoboronate bond.[5] Moreover, *ortho*-hydroxy aldehydes such as pyridoxal or salicylaldehyde (SA) derivatives have been also used to form imines in aqueous media, stabilized by an intramolecular H-bond between the imine *N* atom and the *ortho*-phenolic proton (Figure 1A).[6] Besides their application as site-selective protein and peptide modifiers,[7] the use of SA fragments in the context of RC ligands was firstly described in 2012: a SA-bearing ligand was found to engage a Lys(ε-NH_2) group buried in the RNAse domain of inositol-requiring enzyme 1 endoribonuclease (IRE1).[8] A SA fragment was also installed in the drug GBT440 (Oxbryta™, recently approved for the treatment of sickle cell disease), which prevents the polymerization by forming an imine bond between the SA handle and a N-terminal Val(α-NH_2) group in mutant hemoglobin (HbS).[9] In 2018, Neri and coworkers exploited the SA tag to increase the binding affinity of a group of ligands for their cognate receptors (i.e. albumin, interleukin 2 and urokinase-type plasminogen activator).[10]

It is now clear that SA derivatives are exceptional Lys-engaging agents, capable of forming imine bonds with protein Lys(ε-NH_2) groups with higher efficacy compared to other aldehydes or aminophilic compounds.[12] Very recently, further evidences of the SA-Lys imine bond formation[13] have been provided by the crystal structures of two kinase proteins (BCR-ABL[14] and Aurora A[15]) in complex with SA-bearing inhibitors. Interestingly, no examples of Lys-engaging, SA-equipped peptides have been reported so far in the literature. The design of peptides (i.e. from small linear peptides to large macrocyclic and bicyclic structures) is a well-known strategy to generate

[a] Dr. G. Sacco, Prof. Dr. L. Pignataro, Prof. Dr. L. Belvisi, Dr. A. Dal Corso, Prof. Dr. C. Gennari
Dipartimento di Chimica
Università degli Studi di Milano
via C. Golgi, 19, I-20133, Milan (Italy)
E-mail: alberto.dalcorso@unimi.it
cesare.gennari@unimi.it
[b] Dr. D. Arosio
Istituto di Scienze e Tecnologie Chimiche (SCITEC) "Giulio Natta"
Consiglio Nazionale delle Ricerche
Via Golgi 19, I-20133 Milan (Italy)
[c] Prof. Dr. M. Paolillo
Dipartimento di Scienze del Farmaco
Università degli Studi di Pavia
Viale Taramelli 6, 27100 Pavia (Italy)
[d] Dr. A. Gloger, Dr. J. Scheuermann
Department of Chemistry and Applied Biosciences
ETH Zürich
Vladimir-Prelog-Weg 4, CH-8093 Zürich (Switzerland)

Supporting information for this article is available on the WWW under https://doi.org/10.1002/chem.202203768

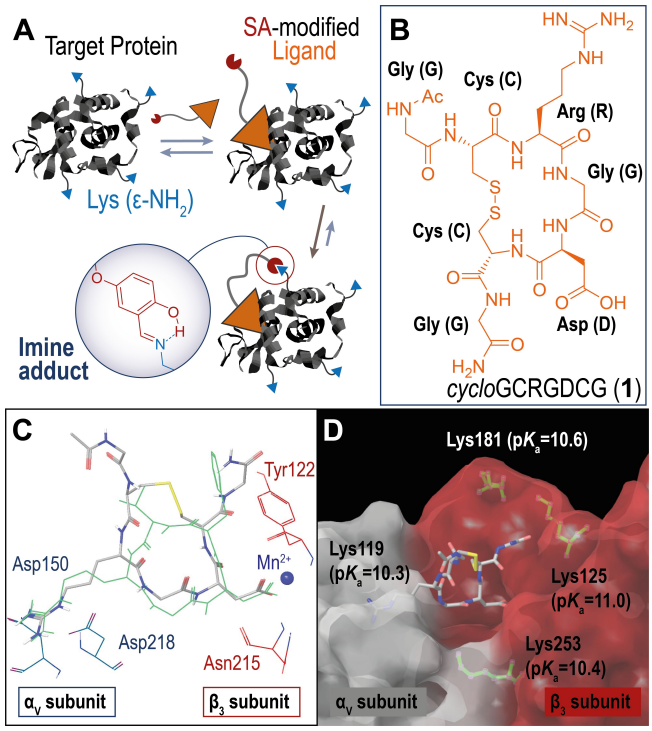

Figure 1. A) Binding mechanism of a RC ligand equipped with a salicylaldehyde (SA) tag. Ideally, SA forms a remarkably stable imine bond with a Lys(ε-NH_2) residue proximal to the ligand binding site. This covalent ligand-protein connection is stabilized by a H bond between the OH phenolic proton and the imine N atom. As a result, the final ligand-protein complex is stabilized by a combination of non-covalent ligand-protein interactions and the covalent imine bond. B) Molecular structure of the integrin-binding *cyclo*GCRGDCG peptide **1**. C) Molecular docking of **1** in the $\alpha_V\beta_3$ crystal structure, overlaid on the bound conformation of the well-known integrin ligand cilengitide[11] (green tube representation, PDB: 1 L5G). D) Four Lys residues are present in the surrounding of the ligand binding site, represented with their pK_a values predicted with the Rosetta webtool (see the Experimental Section).

small ligands against a given protein target.[16] Ideally, the development of SA-equipped peptides would dramatically expand the applications of RC inhibitors, leading to small binders with exceptionally high affinity and selectivity.

Results and Discussion

As a case study to investigate the efficacy of SA-modified peptides, we selected the *cyclo*GCRGDCG peptide (compound **1**, Figure 1B) as small ligand for integrin $\alpha_V\beta_3$, a well-known transmembrane glycoprotein involved in cell adhesion and various signalling cascades.[17] We have recently described the synthesis of **1** and its high affinity for $\alpha_V\beta_3$ ($IC_{50}=6.4$ nM).[18] In this work, we performed molecular docking of **1** in the $\alpha_V\beta_3$ binding site. As shown in Figure 1C, the binding pose of **1** substantially reproduces the ligand-protein interactions observed in the X-ray complex of *cyclo*[RGDf(NMe)V] ligand (Cilengitide).[19]

In particular, the latter binds at the interface of the α_V and β_3 subunits, with the Asp (D) and Arg (R) residues respectively engaging the Mn^{2+} ion in the metal ion-dependent adhesion site (MIDAS) and a negatively charged protein region in an "electrostatic clamp". As shown in Figure 1D, $\alpha_V\beta_3$ features four Lys proximal to the RGD binding site, one in the α_V subunit (Lys119) and three in the β_3 chain (Lys125, 181 and 253). The high exposure to the solvent of all four Lys residues suggested the absence of a hyper-reactive[13] Lys(ε-NH_2) species and this hypothesis was supported by the relatively narrow range of predicted pK_a values ($10.3 < pK_a < 11.0$, Figure 1D) of the four Lys(ε-NH_3^+) groups. Finally, we measured the spatial distance of all four Lys residues from both the N and C termini of peptide **1**, which are exposed to the solvent (see Figure S1 in the Supporting Information file). Lys253 was identified as the closest Lys(ε-NH_2) to the peptide N terminus (7.0–14.4 Å), while Lys125 proved proximal to the C terminus (7.5–8.5 Å). Building on this information, we synthesized two derivatives of peptide **1** (**1-N-SA** and **1-C-SA** in Scheme 1A) bearing the RGD integrin-binding motif, a disulfide bond, and a SA tag, installed either at the peptide N (compound **1-N-SA**) or C (compound **1-C-SA**) termini through a triazole ring. Moreover, two additional peptides (**1-N-BA** and **1-C-BA**, Scheme 1A) were prepared, where the SA tag at the peptide termini was substituted by benzaldehyde (BA), which does not form stable imines in water.[10] Finally, the cyclic pentapeptide **2** (Scheme 1A) was prepared as negative control, in which the Ser-Gly-Glu (SGE) tripeptide was installed in place of the integrin-binding RGD sequence. The negative control **2** was also equipped with the SA tag at the N terminus (**2-N-SA**, Scheme 1A). In order to install the aldehyde tags at the two extremities of the cyclic peptide, we designed two different synthetic routes which are illustrated in Scheme 1B and C. In particular, N-modified peptides (i.e. **1-N-SA**, **1-N-BA** and **2-N-SA**) were rapidly prepared through microwave-assisted solid phase peptide synthesis (SPPS, to give linear peptide **3**, bearing a N-terminal azido group, Scheme 1B), followed by intramolecular disulfide bond formation in solution, using iodine as oxidant. Later on, the resulting cyclic peptide **4** was reacted with SA and BA tags **5**,[10] featuring a terminal alkyne group: copper-catalyzed azide-alkyne cycloaddition (CuAAC) allowed the peptide-tag conjugation, leading to the isolation of final products after HPLC purification and lyophilization. Since the preparation of C-modified peptides on resin is typically cumbersome, we devised the assembly of compounds **1-C-SA** and **1-C-BA** in solution. As shown in Scheme 1C, we started from glycine derivatives **6** and **7** to synthesize peptides **8** (bearing a free carboxylic acid) and **9** (endowed with an amine group and a C-terminal azide). These peptide fragments were coupled to give the protected, linear heptapeptide **10**. Following complete removal of protecting groups from the amino acid side chains under acidic conditions, the azide-bearing peptide was cyclized and conjugated to alkyne through CuAAC, as described above, to give C-tagged peptides **1-C-SA** and **1-C-BA**. All synthetic details and experimental procedures are reported in the Supporting Information file.

The synthesized compounds were tested in vitro for their ability to compete with biotinylated vitronectin for the binding to integrin $\alpha_V\beta_3$ and the resulting IC_{50} values are shown in Table 1. Benzaldehyde-modified ligands **1-N-BA** and **1-C-BA**

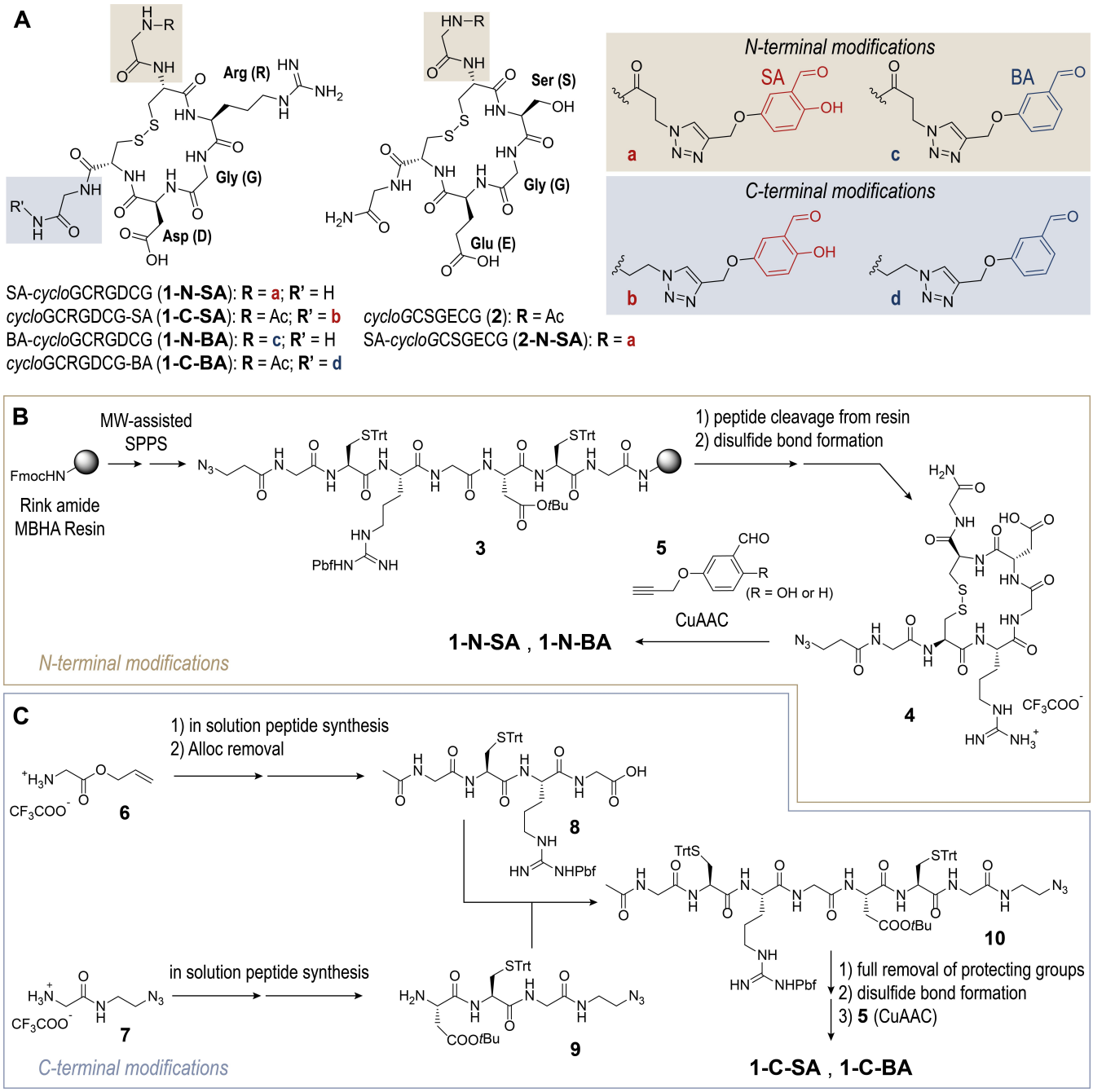

Scheme 1. A) Molecular structures of cyclic peptides bearing salicylaldehyde (SA) or benzaldehyde (BA) modifications at the N (salicylaldehyde in **1-N-SA** and **2-N-SA**, benzaldehyde in **1-N-BA**) or C termini (salicylaldehyde in **1-C-SA**, benzaldehyde in **1-C-BA**). The general synthetic scheme used for the preparation of N-modified (B) and C-modified (C) peptides is also shown. Detailed synthetic procedures are reported in the Supporting Information file. MW: microwave; CuAAC: Copper-catalyzed azide-alkyne cycloaddition.

showed good and very similar binding affinity (IC_{50} values = 6.9 and 7.9 nM respectively), which were comparable to the reported IC_{50} value (6.4 nM) of parent ligand **1**.[18] These data confirmed that the novel triazole connections at both peptide termini are compatible with the RGD binding interactions with the $\alpha_v\beta_3$ pocket. Interestingly, the binding activity of the two salicylaldehyde-modified ligands **1-N-SA** and **1-C-SA** proved very different. Indeed, C-modified peptide **1-C-SA** proved the most active compound of the series (IC_{50} = 3.1 nM). On the other hand, the SA installation at the peptide N terminus proved detrimental for the binding affinity, as ligand **1-N-SA** showed a IC_{50} value in the 10^{-7} M range (129.7 nM), i.e. ca. 20 times higher than the benzaldehyde-bearing compound **1-N-BA** (IC_{50} = 6.9 nM).

Finally, both the negative control SGE peptide **2** and its SA-equipped version **2-N-SA** proved inactive in this experiment

Table 1. Inhibition of biotinylated vitronectin binding to $\alpha_v\beta_3$ integrin mediated by the four aldehyde-modified *cyclo*GCRGDCG peptides.[a]

Modification site	Compound	Sequence	IC_{50} [nM]
N terminus	**1-N-SA**	SA-*cyclo*GCRGDCG	129.7 ± 6.4
	1-N-BA	BA-*cyclo*GCRGDCG	6.9 ± 1.4
C terminus	**1-C-SA**	*cyclo*GCRGDCG-SA	3.1 ± 2.2
	1-C-BA	*cyclo*GCRGDCG-BA	7.9 ± 2.1

[a] IC_{50} values were determined as the concentration of compound required for 50% inhibition of biotinylated vitronectin binding to integrin, as estimated by using GraphPad Prism software. All values are the arithmetic mean ± the standard deviation (SD) of triplicate determinations. A statistical analysis of IC_{50} values is reported in the Supporting Information (Table S2).

(IC_{50} > 1000 nM), confirming that the RGD sequence in peptide-SA adducts is crucial for the integrin binding, and that the SA tag is not active per se in this assay.

The IC_{50} values reported in Table 1 indicate that, depending on the site of installation, the SA tag can enhance or reduce the ability of the cyclic RGD peptide to compete with the natural protein ligand for the same binding pocket. Aiming at a rationale for these observations, we performed covalent docking studies[20] to compare the binding pose of SA-equipped RGD ligands **1-N-SA** and **1-C-SA** in the X-ray structure of $\alpha_v\beta_3$ while forcing a covalent (irreversible) bond between the SA residues and the four Lys groups surrounding the binding site. As summarized in Table S1 (Supporting Information file), this analysis unveiled the potential binding preferences of the two ligands. The forced bond between C-terminal SA in ligand **1-C-SA** and Lys125 proved coherent with the non-covalent interactions of the RGD peptide with the integrin binding pocket. In particular, the cyclic peptide moiety in compound **1-C-SA** overlapped with the Cilengitide structure in the $\alpha_v\beta_3$ binding pocket in 10/10 docking poses (Figure 2A). On the other hand, the anchoring of ligand **1-N-SA** to Lys253 dramatically influenced the non-covalent ligand-protein interactions, forcing the RGD peptide to adopt distorted binding placements in 5/10 docking poses (Figure 2B), that did not match the canonical X-ray Cilengitide pose. These computational analyses are in agreement with the competitive binding studies, as the optimal binding pose of **1-C-SA** is reflected by a lower IC_{50} value compared to control ligand **1-C-BA**. We can also speculate that, upon non-covalent RGD docking, the imine formation between SA of **1-N-SA** and Lys253 destabilizes the cyclopeptide interaction with the protein pocket.

This hypothesis is supported by the very different ability of **1-N-SA** (carrying SA, high IC_{50} value) and **1-N-BA** (carrying BA, low IC_{50} value) to compete with vitronectin for the $\alpha_v\beta_3$ integrin binding site (Table 1).

All in all, information gathered from the binding experiments and the computational studies indicate peptide **1-C-SA** as a novel type of integrin ligand, potentially capable of reversible-covalent interactions with Lys residues. Firstly, docking studies highlighted that the C-terminal triazole-SA moiety may efficiently engage β_3Lys125 in a covalent bond while maintaining the non-covalent interactions between the RGD cyclopeptide and the protein. Moreover, the lower IC_{50} value of ligand **1-C-SA** compared to the benzaldehyde analogue **1-C-BA** indicates a contribution of the *ortho*-phenolic group to the enhanced integrin affinity, presumably by forming an imine-stabilizing H bond (Figure 1A). The relatively small difference of IC_{50} values between **1-C-SA** (3.1 nM) and **1-C-BA** (7.9 nM) may result from a combination of different factors. From the structural viewpoint, a sub-optimal length/flexibility of the triazole-SA tether may hinder the engagement of Lys125, thus limiting the contribution of a stable covalent bond. Moreover, among the four Lys side chains surrounding the integrin binding site (Figure 1D), Lys125(ε-NH_2) was associated to the highest pK_a value (11.0)

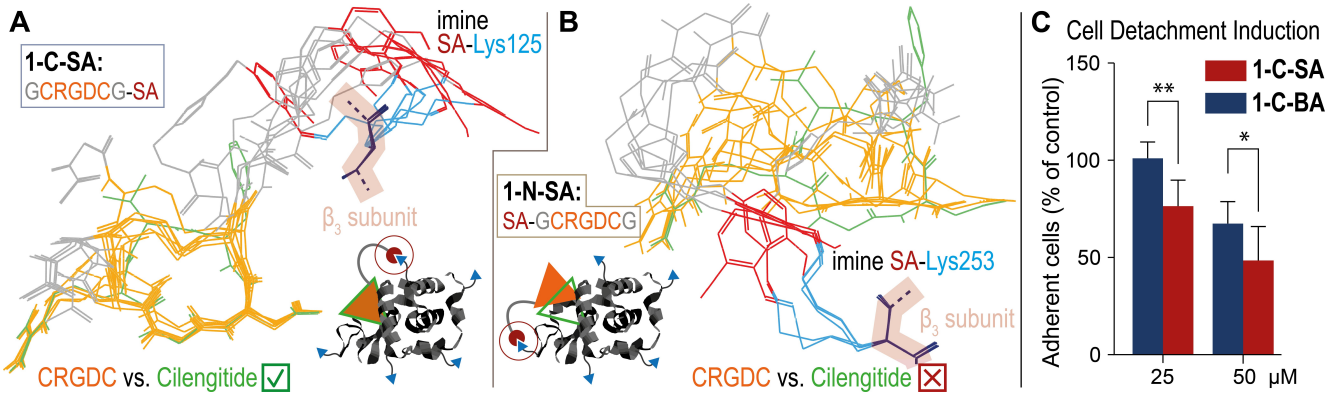

Figure 2. A) Overlay of 10 covalent docking poses of SA-bearing peptide **1-C-SA** where the cyclic peptide (orange) connected to the accessible β3Lys125 (side chain and backbone in light and dark blue, respectively) through the SA tag (red) overlaps with the X-ray structure of benchmark Cilengitide ligand (green). B) Overlay of 5 covalent docking poses of SA-bearing peptide **1-N-SA**, where the forced interaction of N-terminal SA (red) with accessible β3Lys253 (side chain and backbone in light and dark blue, respectively) alters the cyclic peptide (orange) overlapping with Cilengitide (green). C) Induction of cell detachment by *cyclo*GCRGDCG peptides bearing salicylaldehyde (**1-C-SA**) and benzaldehyde (**1-C-BA**) modifications at C-termini. Adherent U-373 MG cells were incubated for 72 h with compounds at 25 or 50 μM concentration. The amounts of adherent cells in the wells were estimated by MTS cell viability assay. The percentage of adherent cells was calculated by normalizing the values with no treatment control. The lines represent mean ± standard deviation. Statistical analysis was performed through paired t test using GraphPad Prism software. * $p < 0.05$, ** $p < 0.005$.

in computational predictions, indicating a high extent of protonation and a weak nucleophilicity.

Finally, to confirm the stronger integrin-binding potency of SA-bearing peptide **1-C-SA** over its BA-modified analogue **1-C-BA** we investigated the ability of the two ligands to bind $\alpha_v\beta_3$ integrin expressed on adherent cells, interfering with cell-adhesion signaling and ultimately leading to cell detachment. Following our reported protocol,[18] U-373 MG cells were incubated with either **1-C-SA** or **1-C-BA** at 25 and 50 μM concentrations. After 72 h, cells were washed, and the amount of live adherent cells was quantified by MTS assay (see the Supporting Information file) and compared to a control group of untreated cells. As shown in Figure 2C, SA-bearing peptide **1-C-SA** induced a significant cell detachment at 25 μM, whereas the BA analogue **1-C-BA** showed no detectable activity at the same concentration. Cell incubation with compounds at 50 μM induced strong cell detachment in both cases, but once again **1-C-SA** proved significantly more active than **1-C-BA**.

Conclusion

This work describes the first example of SA-modified peptides, as a promising strategy to strengthen ligand-protein interactions by reversible-covalent engagement with Lys(ε-NH_2) species. In our study, covalent docking proved to be a valuable tool to rationalize the structure-activity relationships, and it will be important to guide the chemical design of future SA-peptide constructs. The high reactivity of the SA tag towards imine formation and the high frequency of Lys(ε-NH_2) species on the surface of proteins hold promises for the general development of RC inhibitors against a large number of clinically relevant targets and protein-protein interactions.

Experimental Section

The synthetic procedures for the preparation of aldehyde-modified peptides are reported in the Supporting Information file, along with the ^1H and ^{13}C NMR spectra, the HPLC traces and mass spectrometry data.

General Synthetic Procedures

Protocols for semi-automated peptide synthesis: The semi-automated SPPS was carried out using a Biotage Initiator™ synthesizer, assisted by microwave (MW) irradiation. Fmoc/*t*Bu strategy was used for the peptide growth with a Rink amide MBHA resin. Each coupling step consisted in: 1) activation of the Fmoc-protected amino acid; 2) addition of the activated amino acid to the resin at the synthesizer to start the coupling; 3) washing step, Fmoc removal and further washing step. The resin was weighted in a 10 ml Teflon vial (Biotage) and processed through the swelling task: 3 ml of CH_2Cl_2 added to the vial and the mixture was stirred for 20 min at r.t., followed by solvent removal and addition of 3 ml of DMF. The mixture was then stirred at r.t. for 5 min. and the DMF was removed to give swollen beads. Activation of *N*-Fmoc protected amino acids (Fmoc-AA-OH) was performed as follows: a solution of Fmoc-AA-OH (4.0 equiv.) in dry DMF (3 ml) was cooled to 0 °C in an ice bath. HOAt or Oxyma (4.0 equiv.), *i*Pr_2NEt (8.0 equiv.) and DIC (4.0 equiv.) were added to the solution and the mixture was stirred for 15 min at 0 °C. Later on, the reaction mixture was added to the swollen resin (1.0 equiv.) to start the amide coupling reaction. The activated Fmoc-AA-OH residue was added to the resin in the reaction vessel of the synthesizer and the MW-assisted coupling reaction was carried out for 10 min at 75 °C under inert atmosphere. Beads were then washed twelve times with DMF (cycles of 3 ml × 20 sec.) and two Fmoc removal steps were performed by adding a 20 % piperidine solution in DMF (3.0 ml for each step) to the beads: the reaction was performed at r.t. under inert atmosphere for 2 min and 10 min for the first and the second Fmoc removal step, respectively. The beads were washed with DMF (×6), CH_2Cl_2 (×2) and again DMF (2×3.0 ml for 20 sec.). following these washout steps, the following coupling reaction was performed. Whenever the peptide synthesis was interrupted, the resin was dried with Et_2O (3 ml) and the suspension was stirred for 1 min at r.t. The beads were washed with further Et_2O (6×3.0 ml for each wash, 5× 45 sec. and, for the last one, 1×30 sec with a 2 min draining). Peptides on resin were stored at −20 °C after drying with Et_2O. The subsequent SPPS cycle was started again with a swelling step before continuing with the peptide synthesis.

General procedure A for simultaneous peptide cleavage and side-chain protecting group removal: Peptide cleavage from resin was performed manually, under inert atmosphere and vortex mixing. The on-beads protected peptide was swollen with DMF (3 ml), followed by CH_2Cl_2 (3 ml). Under stirring and nitrogen atmosphere, the beads were treated three times (3.0 ml for 0.1 mmol of resin) with a 95 : 2,5 : 2,5 TFA/TIS/H_2O (*v/v/v*) cleavage cocktail solution. After 1 h, the liquid phase was filtered off under nitrogen flow and collected in a round bottom flask: the beads were washed with neat TFA (1.0 ml) and the liquid layer was collected. The combined liquid layers were concentrated under rotary evaporation and poured in ice-cold Et_2O, leading to precipitation of a white solid. Et_2O was removed with centrifugation and the white pellet was purified by HPLC.

General Procedure B for Intramolecular Disulfide Bond Formation: In a round-bottom flask, the linear peptide (1 eqiv.) was dissolved in a 1 : 1 H_2O/MeCN mixture (2 mM). I_2 (20 equiv.) was added to the solution and the mixture was stirred for 30 minutes at r.t. The reaction mixture was concentrated and the resulting crude was purified by HPLC. The pure cyclized peptide was isolated after lyophilization.

General procedure C for protecting group removal from peptide: In a round-bottom flask, a 95 : 2.5 : 2.5 TFA:TIS:H_2O mixture was added to the cyclic protected peptide (1.0 equiv.) at 0 °C (0.02 M concentration). The reaction mixture was stirred at r.t. for 2 h, concentrated in vacuo and diluted with cold Et_2O, leading to the formation of a white precipitate. The crude was isolated by centrifugation and the resulting solid was used in the following synthetic steps.

General procedure D for CuAAC reaction: A stock solution of the azide (0.1 M in degassed water, 1 equiv.) and alkyne (0.1 M in degassed DMF, 1.3 equiv.) were added to a flask under a nitrogen atmosphere. To this mixture, a stock solution of $CuSO_4 \cdot 5H_2O$ (0.1 M in degassed water, 1 equiv.) and sodium ascorbate (0.1 M in degassed water, 1.1 equiv.) were sequentially added and the reaction mixture was stirred at 40 °C overnight. The reaction mixture was dried in vacuo and the resulting crude was purified by RP-HPLC.

General procedure E for amide coupling in solution: A 0.2 M solution of Fmoc-AA-OH (1.1 equiv.) in dry DMF was cooled to 0 °C under a nitrogen atmosphere. To this solution, HATU (1.1 equiv), HOAt (1.1 equiv.) and *i*Pr_2NEt (3 equiv.) were added sequentially, and the

resulting solution was stirred at 0 °C for 15 min. The amine (1 equiv.) was then added to the previously obtained solution and the reaction mixture was stirred at r.t. overnight. The mixture was concentrated in vacuo and the resulting crude was dissolved in AcOEt. The organic phase was washed once with aqueous 1 M $KHSO_4$, once with sat. aq. $NaHCO_3$, once with brine. The organic layer was dried and concentrated, and the crude product was purified with flash chromatography to give the desired amide.

General procedure F for Fmoc removal in solution: N-Fmoc protected compound (1 equiv.) was dissolved at 0.1 M concentration in a 1:1 diethylamine/MeCN mixture. The resulting solution was stirred at r.t and the starting material consumption was followed by TLC. The reaction mixture was concentrated, the resulting crude was co-evaporated three times with MeCN to remove the traces of diethylamine. The crude was filtered over a pad of silica (first elution with 1:1 AcOEt/Hex, followed by amine elution with 10% MeOH in CH_2Cl_2 + 1% Et_3N) and then used as starting material for the following synthetic step.

Computational Studies

All calculations were performed using the Schrödinger Suite through the Maestro graphical interface [Maestro, version 10.5, Schrödinger, LLC, New York, NY, 2016].

Ligand preparation: Ionized carboxylate and protonated guanidinium groups have been employed in calculations for the cyclic RGD integrin ligands as the relevant protonation states at pH = 7 for the acid and basic pharmacophoric groups according to Epik module [Epik version 3.5, Schrödinger, LLC, New York, NY, 2016]. The conformation in water solution of a *cyclo*(CRGDC) derivative was previously investigated by NMR spectroscopy and MD simulations.[21] NMR and computational studies indicate flexibility of the macrocycle yet providing support for an extended conformation of the RGD sequence and for the presence of an inverse γ-turn centered on residue Asp of the ligand. In addition, although the inverse γ-turn conformation is not highly populated in the free peptide, the receptor-bound ligand, similarly to Cilengitide in the $\alpha_v\beta_3$-bound X-ray structure, adopts this conformation in docking models to optimize the interactions with the integrin.[21] Accordingly, macrocycle conformations of the new *cyclo*GCRGDCG ligands (**1**, **1-N-SA**, **1-C-SA**) resembling the X-ray $\alpha_v\beta_3$-bound geometry of Cilengitide have been employed in docking calculations (i.e. extended conformation of the RGD sequence and inverse γ-turn centered on Asp residue).

Protein preparation: The crystal structure of the extracellular domain of the integrin $\alpha_v\beta_3$ in complex with the cyclic pentapeptide RGDf(NMe)V Cilengitide (PDB code 1 L5G) was used for docking studies. The $\alpha_v\beta_3$ integrin structure was set up for docking as previously reported (residues 1–438 for chain α_v and 107–354 for chain β_3, all bivalent cations modeled as Mn^{2+} ions).[22] Then, the Protein Preparation Wizard using the OPLS2005 force field was run to get the final structures.

Molecular docking: Conventional non-covalent docking calculations were performed using Glide version 7.0 [Glide version 7.0, Schrödinger, LLC, New York, NY, 2016] in the SP (Standard Precision) mode to produce initial docking poses. Receptor grids were generated on the extracellular fragments of $\alpha_v\beta_3$ integrin prepared as described in section "*Protein preparation*". The settings of the flexible-ligand docking protocol were defined as previously reported.[22] The docking protocol was also tested for its ability to reproduce the X-ray binding mode of the cyclic RGD ligand in the receptor crystal structure. Glide was successful in reproducing the experimentally determined binding mode of the cyclic peptide Cilengitide in $\alpha_v\beta_3$ integrin, as it corresponds to the best-scored poses in the docking run. Non-covalent docking poses of the new *cyclo*GCRGDCG ligands show that the RGD peptide can reproduce the X-ray binding mode, and the salicylaldehyde (SA) handle either at the peptide N terminus (**1-N-SA**) or C terminus (**1-C-SA**) can fit unhindered in the $\alpha_v\beta_3$ binding site without forming specific interactions with integrin residues.

The covalent docking protocol available in the Schrödinger Suite [Covalent Docking v1.2, Glide, version 7.0, Schrödinger, LLC, New York, NY, 2016] was then applied to generate binding poses of **1-N-SA** and **1-C-SA** in the X-ray structure of $\alpha_v\beta_3$ while forcing the covalent bond between the SA moieties and the most accessible Lys(ε-NH_2) groups of both integrin subunits (i.e. α_vLys119, β_3Lys125, β_3Lys181, and β_3Lys253, Figure S1).[20] The docked ligands were confined to an enclosing box with box center in the ligand centroid and automatic box size. A custom imine condensation reaction type was defined to select only aldehyde moieties as reactive sites. Further settings include: docking mode in pose prediction, affinity score calculation using Glide, 10 output poses per ligand reactive site.

Analysis of the covalently bound complexes focused on the ability of the cyclic peptides to maintain the canonical X-ray non-covalent interactions of the RGD peptide in the binding pocket while forming the covalent imine bond with a Lys residue. The results of this analysis are shown in Figure 2 and in Table S1.

Calculation of protein pK_a values: The pK_a values of integrin Lys(ε-NH_2) groups were predicted with the Rosetta webtool using the PDB 1 L5G $\alpha_v\beta_3$ crystal structure.[23] The results of the Lys(ε-NH_2) groups of both integrin subunits, proximal to the ligand binding site, are shown in Figure 1D.

Protocols for Biological Evaluations

Solid phase receptor binding assays: Recombinant human integrin $\alpha_v\beta_3$ receptor (R&D Systems, Minneapolis, MN, USA) was diluted to 0.5 μg/ml in coating buffer containing 20 mM Tris-HCl (pH 7.4), 150 mM NaCl, 1 mM $MnCl_2$, 2 mM $CaCl_2$, and 1 mM $MgCl_2$. An aliquot of diluted receptor (100 μL/well) was added to 96-well microtiter plates (Nunc MaxiSorp) and incubated overnight at 4 °C. The plates were then washed and incubated with blocking solution (20 mM HEPES (pH 7.5), 150 mM NaCl, 1 mM $MnCl_2$, 2 mM $CaCl_2$, and 1 mM $MgCl_2$, plus 1% bovine serum albumin) for 2 h at r.t. to block nonspecific binding. After washing 2 times with blocking solution, plates were incubated shaking for 3 h at r.t., with various concentrations (10^{-5}–10^{-12} M) of test compounds 1-N-SA, 1-C-SA, 1-N-BA, 1-C-BA, 2, 2-N-SA in the presence of 1 μg/ml biotinylated vitronectin (Molecular Innovations, Novi, MI, USA). Biotinylation was performed using an EZ-Link Sulfo-NHS-Biotinylation kit (Pierce, Rockford, IL, USA). After washing 3 times, the plates were incubated shaking for 1 h at r.t., with streptavidin-biotinylated peroxidase complex (Amersham Biosciences, Uppsala, Sweden). After washing 3 times with blocking solution, plates were incubated in the dark with 100 μL/well of Substrate Reagent Solution (R&D Systems, Minneapolis, MN, USA) for 30 min with shaking. After stopping the reaction with 50 μL/well 2 N H_2SO_4, absorbance at 415 nm was read in a SynergyTM HT Multi-Detection Microplate Reader (BioTek Instruments, Inc.). Each data point represents the average of triplicate wells; data analysis was carried out by nonlinear regression analysis with GraphPad Prism software (GraphPad Prism, San Diego, CA, USA). Each experiment was repeated in triplicate.

Cell culture: The U-373 MG human glioblastoma cell lines were purchased from Istituto Zootecnico Regione Lombardia (Brescia, Italy). The cell lines were grown in DMEM supplemented with 5% fetal bovine serum (FBS), 2 mM glutamine, penicillin-streptomycin (10000 u/ml) and cells were grown at 37 °C in controlled

atmosphere (5% CO_2/95% air). Confluent cells were split (1:5–1:10 ratio) by trypsinization and used at the third-fourth passage after thawing. For all the experiments the cells were plated at a density of 10000 cells/cm^2. The reagents used for the cell cultures were from Euroclone, Italy.

Cell detachment assays: Cells plated in 96 multiwells in the growth medium (10.000 cells/100 μl per well) were treated with cell culture medium containing 0, 25 and 50 μM concentrations of compounds **1-C-SA** and **1-C-BA** for 72 h. Stock solutions of compound **1-C-SA** and **1-C-BA** (200 mM in PBS) were diluted in the growth medium and added to the wells. In control wells only the growth medium was added. At the end of treatments, wells were rinsed three times with PBS and floating cells were separated. The viability of adherent cells was measured in by adding 20 μl of MTS reagent (CellTiter 96 AQueous One Solution Cell Proliferation Assay, Promega) to each well. After incubation for 3 h under standard conditions, the absorbance was read in a multiwell plate reader at 450 nm. Six wells were used for each experimental point and each independent experiment was performed three times. Similarly, the separated population of floating cells was subjected to a second MTS assay, which confirmed the viability of detached cells.

Acknowledgements

We gratefully acknowledge Ministero dell'Università e della Ricerca (PRIN 2020 project 2020833Y75) for financial support. High-resolution mass spectrometry analyses were performed at the MS facility of the Unitech COSPECT at the University of Milan (Italy). Open Access funding provided by Università degli Studi di Milano within the CRUI-CARE Agreement.

Conflict of Interest

The authors declare no conflict of interest.

Data Availability Statement

The data that support the findings of this study are available in the supplementary material of this article.

Keywords: aldehydes · cell adhesion · covalent inhibitors · integrins · peptidomimetics

[1] S. M. Hacker, *Nature* **2022**, *603*, 583–504.
[2] H. Zhang, W. Jiang, P. Chatterjee, Y. Luo, *J. Chem. Inf. Model.* **2019**, *59*, 2093–2102.
[3] a) K. Senkane, E. V. Vinogradova, R. M. Suciu, V. M. Crowley, B. W. Zaro, J. M. Bradshaw, K. A. Brameld, B. F. Cravatt, *Angew. Chem. Int. Ed.* **2019**, *58*, 11385–11389; *Angew. Chem.* **2019**, *131*, 11507–11511; b) N. Shindo, H. Fuchida, M. Sato, K. Watari, T. Shibata, K. Kuwata, C. Miura, K. Okamoto, Y. Hatsuyama, K. Tokunaga, S. Sakamoto, S. Morimoto, Y. Abe, M. Shiroishi, J. M. M. Caaveiro, T. Ueda, T. Tamura, N. Matsunaga, T. Nakao, S. Koyanagi, S. Ohdo, Y. Yamaguchi, I. Hamachi, M. Ono, A. Ojida, *Nat. Chem. Biol.* **2019**, *15*, 250–258; c) Z. Zhou, X. Chen, Y. Fu, Y. Zhang, S. Dai, J. Li, L. Chen, G. Xu, Z. Chen, Y. Chen, *Chem. Commun.* **2019**, *55*, 5890–5893; d) W.-H. Guo, X. Qi, X. Yu, Y. Liu, C.-I Chung, F. Bai, X. Lin, D. Lu, L. Wang, J. Chen, L. H. Su, K. J. Nomie, F. Li, M. C. Wang, X. Shu, J. N. Onuchic, J. A. Woyach, M. L. Wang, J. Wang, *Nat. Commun.* **2020**, *11*, 4268; e) R. Gabizon, A. Shraga, P. Gehrtz, E. Livnah, Y. Shorer, N. Gurwicz, L. Avram, T. Unger, H. Aharoni, S. Albeck, A. Brandis, Z. Shulman, B.-Z. Katz, Y. Herishanu, N. London, *J. Am. Chem. Soc.* **2020**, *142*, 11734–11742.
[4] S. Gardini, S. Cheli, S. Baroni, G. Di Lascio, G. Mangiavacchi, N. Micheletti, C. L. Monaco, L. Savini, D. Alocci, S. Mangani, N. Niccolai, *PLoS One* **2016**, *11*, e0148174.
[5] a) P. M. S. D. Cal, J. B. Vicente, E. Pires, A. V. Coelho, L. F. Veiros, C. Cordeiro, P. M. P. Gois, *J. Am. Chem. Soc.* **2012**, *134*, 10299–10305; b) G. Akçay, M. A. Belmonte, B. Aquila, C. Chuaqui, A. W. Hird, M. L. Lamb, P. B. Rawlins, N. Su, S. Tentarelli, N. P. Grimster, Q. Su, *Nat. Chem. Biol.* **2016**, *12*, 931–936; c) D. Quach, G. Tang, J. Anantharajan, N. Baburajendran, A. Poulsen, J. L. K. Wee, P. Retna, R. Li, B. Liu, D. H. Y. Tee, P. Z. Kwek, J. K. Joy, W.-Q. Yang, C.-J. Zhang, K. Foo, T. H. Keller, S. Q. Yao, *Angew. Chem. Int. Ed.* **2021**, *60*, 17131–17137; *Angew. Chem.* **2021**, *133*, 17268–17274; d) R. M. Reja, W. Wang, Y. Lyu, F. Haeffner, J. Gao, *J. Am. Chem. Soc.* **2022**, *144*, 1152–1157.
[6] G. Sacco, S. Stammwitz, L. Belvisi, L. Pignataro, A. Dal Corso, C. Gennari, *Eur. J. Org. Chem.* **2021**, *2021*, 1763–1767.
[7] a) C. B. Rosen, M. B. Francis, *Nat. Chem. Biol.* **2017**, *13*, 697–705; b) S. R. Adusumalli, D. G. Rawale, U. Singh, P. Tripathi, R. Paul, N. Kalra, R. K. Mishra, S. Shukla, V. Rai, *J. Am. Chem. Soc.* **2018**, *140*, 15114–15123; c) S. R. Adusumalli, D. G. Rawale, K. Thakur, L. Purushottam, N. C. Reddy, N. Kalra, S. Shukla, V. Rai, *Angew. Chem. Int. Ed.* **2020**, *59*, 10332–10336; *Angew. Chem.* **2020**, *132*, 10418–10422; d) A. Märcher, J. Palmfeldt, M. Nisavic, K. V. Gothelf, *Angew. Chem. Int. Ed.* **2021**, *60*, 6539–6544; *Angew. Chem.* **2021**, *133*, 6613–6618; e) M. J. S. A. Silva, R. A. N. Cavadas, H. Faustino, L. F. Veiros, P. M. P. Gois, *Chem. Eur. J.* **2022**, *28*, e202202377.
[8] A SA-bearing small molecule was found to engage a lysine side chain buried in the RNAse domain of IRE1, see: B. C. S. Cross, P. J. Bond, P. G. Sadowski, B. Kant Jha, J. Zak, J. M. Goodman, R. H. Silverman, T. A. Neubert, I. R. Baxendale, D. Ron, H. P. Harding, *Proc. Natl. Acad. Sci. USA* **2012**, *109*, E869.
[9] D. Oksenberg, K. Dufu, M. P. Patel, C. Chuang, Z. Li, Q. Xu, A. Silva-Garcia, C. Zhou, A. Hutchaleelaha, L. Patskovska, Y. Patskovsky, S. C. Almo, U. Sinha, B. W. Metcalf, D. R. Archer, *Br. J. Haematol.* **2016**, *175*, 141–153.
[10] A. Dal Corso, M. Catalano, A. Schmid, J. Scheuermann, D. Neri, *Angew. Chem. Int. Ed.* **2018**, *57*, 17178–17182; *Angew. Chem.* **2018**, *130*, 17424–17428.
[11] C. Mas-Moruno, F. Rechenmacher, H. Kessler, *Adv. Anticancer Agents Med. Chem.* **2010**, *10*, 753–768.
[12] a) M. Wolter, D. Valenti, P. J. Cossar, L. M. Levy, S. Hristeva, T. Genski, T. Hoffmann, L. Brunsveld, D. Tzalis, C. Ottmann, *Angew. Chem. Int. Ed.* **2020**, *59*, 21520–21524; *Angew. Chem.* **2020**, *132*, 21704–21708; b) M. E. Abbasov, M. E. Kavanagh, T. Ichu, M. R. Lazear, Y. Tao, V. M. Crowley, C. W. am Ende, S. M. Hacker, J. Ho, M. M. Dix, R. Suciu, M. M. Hayward, L. L. Kiessling, B. F. Cravatt, *Nat. Chem.* **2021**, *13*, 1081–1092.
[13] The susceptibility of Lys(ε-NH_2) to form covalent bonds is often described in terms of pK_a values. Since Lys(ε-NH_2) is typically protonated under physiological pH (pK_a = 10.4 of the corresponding ammonium ion), solvent-exposed residues typically show low nucleophilicity. However, different structural or mechanical aspects in proteins or in protein-protein interfaces can sensibly decrease the amine pK_a (down to 5 units), enhancing its nucleophilicity. These pK_a-perturbed residues are often referred to as hyper-reactive, see ref. [12b] and J. Pettinger, K. Jones, M. D. Cheeseman, *Angew. Chem. Int. Ed.* **2017**, *56*, 15200–15209; *Angew. Chem.* **2017**, *129*, 15398–15408.
[14] P. Chen, J. Sun, C. Zhu, G. Tang, W. Wang, M. Xu, M. Xiang, C.-J. Zhang, Z.-M. Zhang, L. Gao, S. Q. Yao, *Angew. Chem. Int. Ed.* **2022**, *61*, e202203878; *Angew. Chem.* **2022**, *134*, e202203878.
[15] T. Yang, A. Cuesta, X. Wan, G. B. Craven, B. Hirakawa, P. Khamphavong, J. R. May, J. C. Kath, J. D. Lapek, S. Niessen, A. L. Burlingame, J. D. Carelli, J. Taunton, *Nat. Chem. Biol.* **2022**, *18*, 934–941.
[16] a) A. Zorzi, K. Deyle, C. Heinis, *Curr. Opin. Chem. Biol.* **2017**, *38*, 24–29; b) B. M. Cooper, J. Iegre, D. H. O'Donovan, M. Ölwegård Halvarsson, D. R. Spring, *Chem. Soc. Rev.* **2021**, *50*, 1480–1494.
[17] R. J. Slack, S. J. F. Macdonald, J. A. Roper, R. G. Jenkins, R. J. D. Hatley, *Nat. Rev. Drug Discovery* **2022**, *21*, 60–78.
[18] G. Sacco, A. Dal Corso, D. Arosio, L. Belvisi, M. Paolillo, L. Pignataro, C. Gennari, *Org. Biomol. Chem.* **2019**, *17*, 8913–8917.
[19] J.-P. Xiong, T. Stehle, R. Zhang, A. Joachimiak, M. Frech, S. L. Goodman, M. A. Arnaout, *Science* **2002**, *296*, 151–155.
[20] K. Zhu, K. W. Borrelli, J. R. Greenwood, T. Day, R. Abel, R. S. Farid, E. Harder, *J. Chem. Inf. Model.* **2014**, *54*, 1932–1940.

[21] A. Spitaleri, S. Mari, F. Curnis, C. Traversari, R. Longhi, C. Bordignon, A. Corti, G. Rizzardi, G. Musco, *J. Biol. Chem.* **2008**, *283*, 19757–19768.
[22] L. Ferrazzano, D. Corbisiero, E. Potenza, M. Baiula, S. D. Dattoli, S. Spampinato, L. Belvisi, M. Civera, A. Tolomelli, *Sci. Rep.* **2020**, *10*, 7410.
[23] a) K. P. Kilambi, J. J. Gray, *Biophys. J.* **2012**, *103*, 587–595; b) S. Lyskov, F.-C. Chou, S. O. Conchfflir, B. S. Der, K. Drew, D. Kuroda, J. Xu, B. D. Weitzner, P. D. Renfrew, P. Sripakdeevong, B. Borgo, J. J. Havranek, B. Kuhlman, T. Kortemme, R. Bonneau, J. J. Gray, R. Das, *PLoS One* **2013**, *8*, e63906.

Manuscript received: December 2, 2022
Accepted manuscript online: January 3, 2023
Version of record online: February 27, 2023